

Two Pillared Metal–Organic Frameworks Comprising a Long Pillar Ligand

Hosein Ghasempour,^a Alireza Azhdari Tehrani,^a Ali Morsali,^{*a} Jun Wang,^b and Peter C. Junk^b

^a Department of Chemistry, Faculty of Sciences, Tarbiat Modares University, P.O. Box 14115-175, Tehran, Iran

^b College of Science Technology and Engineering, James Cook University, Townsville Qld, 4811, Australia

Experimental Section.....	page 2
Computational Details.....	page 2
Single Crystal Diffraction.....	page 3
Synthesis and activation of TMU-25 and TMU-26.....	page 4
Fluorescence measurements.....	page 6
Knoevenagel condensation Reaction.....	page 6
Thermogravimetric analysis of TMU-25 and TMU-26.....	page 8
FT-IR spectra of TMU-25 and TMU-26.....	page 9
PXRD patterns of TMU-25 and TMU-26.....	page 10
Fluorescence emission spectra of TMU-25 in different solvents.....	page 11
Solid state photoluminescence spectra of TMU-25 and TMU-26.....	page 12
Fluorescence emission spectra of TMU-25 in benzene, toluene, nitrobenzene.....	page 13
Fluorescence emission spectra of TMU-25 and TMU-26 in different concentrations of nitrobenzene.....	page 14
Comparison of Stern–Volmer (SV) plots of TMU-25 and TMU-26	page 15
Fluorescence emission spectra of TMU-25 and TMU-25 in different aromatic hydrocarbons.....	page 16
Comparative PXRD patterns of TMU-25 as-synthesized and the recycled one.....	page 18
Comparative FT-IR patterns of TMU-25 as-synthesized and the recycled one.....	page 19
Reusability of TMU-25 in Knoevenagel condensation reaction.....	page 19
π–π stacking interactions between parallel L pillar ligands coordinated to two adjacent metal centers in TMU-25 and TMU-26.....	page 20
Relative contributions of various non-covalent contacts to the Hirshfeld surface area in compounds TMU-25 and TMU-26.	page 20
References	page 21

Experimental Section

Materials and Physical Techniques

Zinc (II) nitrate hexahydrate, Cadmium (II) nitrate dihydrate and 2-Aminoterephthalic acid ($\text{NH}_2\text{-BDC}$) were purchased from Aldrich and Merck Company and used as received. Melting points were measured on an Electrothermal 9100 apparatus. IR spectra were recorded using Thermo Nicolet IR 100 FT-IR. The thermal behavior was measured with a PL-STA 1500 apparatus with the rate of $10^\circ\text{C}\cdot\text{min}^{-1}$ in a static atmosphere of argon. X-ray powder diffraction (XRD) measurements were performed using a Philips X'pert diffractometer with mono chromated $\text{Cu-K}\alpha$ radiation. Photoluminescence (PL) measurements were performed by exciting with a high pressure Hg lamp and using a 360 nm filter, the emission of the solutions was collected through an optical fiber and measured using an Avantes spectrometer (AvaSpec-2048 TEC)

Computational Details

Time-dependent density functional theory (TD-DFT) calculations were performed using GAMESS suite of program. The organic linkers of TMU-25 and TMU-26 were optimized at B3LYP/6-311g(d,p) level of theory. Frontier molecular orbitals were calculated for nitrobenzene, benzene, toluene and the organic linkers using TD-DFT calculations at the B3LYP/6-311g(d,p) basis set for all atoms. Frontier MOs were plotted at an isovalue of 0.02 au.

Hirshfeld Surface Analysis:

The intermolecular interactions in the crystal structures of compounds **TMU-25** and **TMU-26** are quantified via Hirshfeld surface analysis using CrystalExplorer 3.0. These surfaces visually

summarize the spatial arrangement and relevance of intermolecular interactions by their color code.

Single-Crystal Diffraction.

X-ray crystal structure determinations: Crystals in viscous paraffin oil were mounted on cryoloops and intensity data were collected on the Australian Synchrotron MX1 beamline at 100 K with wavelength ($\lambda = 0.71073 \text{ \AA}$). The data were collected using the BlueIce[1] GUI and processed with the XDS[2] software package. The structures were solved by conventional methods and refined by full-matrix least-squares on all F^2 data using SHELX97[3] or SHELX2014 in conjunction with the X-Seed[4] or Olex2[5] graphical user interface. Anisotropic thermal parameters were refined for non-hydrogen atoms and hydrogen atoms were calculated and refined with a riding model. The crystals were twinned and these data sets are the best that have been collected and no more stable refinements can be achieved from the data. For TMU-25 and TMU-26 $C_{38}H_{37}N_7O_6Zn$ and $C_{38}H_{37}N_7O_6Cd$ calculated formula by SQUEEZE/PLATON are consistent with that of $[Zn(NH_2-bdc)(L)].2DMF$ and $Cd(NH_2-bdc)(L)].2DMF$, respectively.

2. Experimental

Synthesis procedures

Synthesis of N_4,N_4 -bis(pyridin-4-ylmethylene)-[1,1'-biphenyl]-4,4'-diamine (L): N^4,N^4 -bis(pyridin-4-ylmethylene)-[1,1'-biphenyl]-4,4'-diamine (L), as a ligand, was synthesized according to the following procedure.

First, 1.81 g of benzidine (5 mmol) was dissolved in ethanol (15 mL). Then, 0.94 mL of pyridine-4-carboxaldehyde (10 mmol) was added to the solution. Afterward, two drops of formic acid were added and the mixture was stirred for two hours at room temperature. The deposit was a yellow solid which was filtered and washed several times with ethanol. Yield, 79%, m.p = 258-260 °C, FT-IR peaks (cm^{-1}): 3421 (s), 1619 (s), 1600 (s), 1550 (s), 1487 (m), 1408 (s), 1321 (w), 1217 (m), 1122(w), 974 (w), 820 (vs), 649 (m), 540 (s).

Synthesis of $[\text{Zn}(\text{NH}_2\text{-bdc})(\text{L})]\cdot 2\text{DMF}$ (TMU-25)

0.298 g of $\text{Zn}(\text{NO}_3)_2 \cdot 6\text{H}_2\text{O}$ (1 mmol), 0.181 g of synthesized 4-bpmbp (0.5 mmol), 0.181 g of 2-Aminoterephthalic acid (1 mmol) were first dissolved in 15 ml of DMF (N,N' -Dimethylformamide). The mixture was then placed in a Teflon reactor and heated at 90 °C for 3 days. The mixture was then gradually cooled to room temperature during 24 hours. Brown crystals were formed on the walls of reactor with a 38% synthesis yield. Calculated elemental analysis data of TMU-25 (%): C: 61.82; H: 4.45; N: 12.36. Measured data (%): C: 62.12; H: 4.48; N: 12.75. m.p > 350° C, FT-IR selected peaks (cm^{-1}): 3445 (m), 3349 (m), 2924 (m) 1672 (s), 1608 (s), 1575 (vs), 1427 (m), 1375 (vs), 1254 (s), 1092 (m), 830 (s), 767 (s), 659 (m), 549 (m). The symmetric and asymmetric vibrations of the carboxylate group are observed as two strong bands at 1427 and 1575 cm^{-1} , respectively. The bands at 3445 and 3349 cm^{-1} are related to

amine group in NH₂-BDC ligand. Also the weak band at 2924 cm⁻¹ can be related to aliphatic C-H of Schiff-base bond in L ligand. For activation purpose, synthesized crystals were then soaked in a 5 mL of CHCl₃ solvent for 5 days, with fresh CHCl₃ added every 24 hours. After 5 days the CHCl₃ solution was decanted, and activated crystals were dried at 100 °C under vacuum for at least 24 hours.

Synthesis of [Cd(NH₂-bdc)(L)].2DMF (TMU-26)

0.308 g of Cd(NO₃)₂.2H₂O (1 mmol), 0.181 g of synthesized 4-bpmbp (0.5 mmol), 0.181 g of NH₂-bdc (1 mmol) were dissolved in 15 ml of DMF. The mixture was then placed in a Teflon reactor and heated at 90 °C for 3 days, and was gradually cooled to room temperature during 24 hours. The yellow needle-shaped crystals were obtained from walls of reactor with a 31% synthesis yield. Calculated elemental microanalysis data of synthesized TMU-26 (%): C: 57.82; H: 4.16; N: 11.56. Measured data (%): C: 57.75; H: 4.10; N: 11.48. m.p > 350° C, FT-IR selected peaks (cm⁻¹): 3428 (m), 3341 (s), 2926 (m), 1672 (s), 1611 (s), 1557 (vs), 1496 (m), 1371 (vs), 1258 (m), 1092 (m), 1009 (w), 831 (s), 773 (m), 660 (m), 548 (m). The symmetric and asymmetric vibrations of the carboxylate group are observed as two strong bands at 1496 and 1557 cm⁻¹, respectively. The bands at 3428 and 3341 cm⁻¹ are related to amine group in NH₂-BDC ligand. Also the weak band at 2926 cm⁻¹ can be related to aliphatic C-H of Schiff-base bond in L ligand. The same procedure was used for the activation of TMU-26. The PXRD results, however, revealed that TMU-26 was not stable and its structure collapsed after activation.

Fluorescence Measurements

The Fluorescence properties of synthesized MOFs were measured in the solid state and in different solvent emulsions using a PerkinElmer-LS55 Fluorescence Spectrometer at room temperature. In a typical procedure, 1 mg of synthesized MOFs was grinded down, and then immersed in different organic solvents (2.5 ml) and after 24 hours was tested in the emission mode. In addition, TMU-25 and TMU-26 are also responding to benzene, naphthalene and anthracene. For fluorescence measurement in the presence of PAHs, toluene was chosen as suitable solvent because naphthalene and anthracene are soluble in it and stable emulsion containing MOF is formed. As expected, the emission band is red-shifted in going from benzene to anthracene.

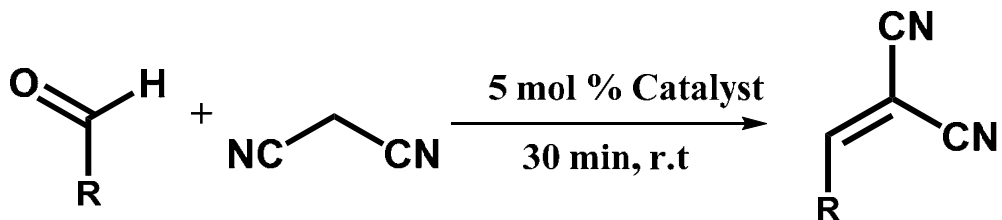
Stern-Volmer Plots

According to the Stern-Volmer equation, $(I_0/I) = K_Q [A] + 1$, Where here, I_0 is the initial fluorescence intensity of soaked MOF sample in toluene, I is the fluorescence intensity in the presence of nitrobenzene, $[A]$ is the molar concentration of nitrobenzene, and K_Q is the quenching constant (M^{-1}). For the quenching constant extraction, emission intensity of all MOFs was recorded by suspending them into different concentrations of nitrobenzene solutions in toluene, upon the same manner described in Fluorescence measurement section.

Knoevenagel condensation Reaction

17 mg (5 mol%) of solid MOF catalyst was added into the reaction vessel loaded with a mixture of malononitrile (1.1 mmol) and benzaldehyde (1.0 mmol), in 3 ml Solvent. The resulting mixture was stirred at room temperature for 30 minutes. The reaction progress was followed by GC analysis. For this, the reaction mixture was centrifuged and the solid catalyst was filtered off.

Then the reaction mixture passed through the 0.4μ filter and subsequently analyzed by GC analysis using an internal-standard method.



Catalyst Recycling

The reusability of this catalyst, was tested for the condensation reaction in the presence of two fold amounts of the catalysts (5 mol%, 35 mg), benzaldehyde (2 mmol) and malononitrile (2.1 mmol). After 30 minutes, the heterogeneous mixture was allowed to settle completely followed by decanting the supernatant liquid. The catalyst was washed with excess MeOH and the reaction vessel containing the washed recycled catalyst was loaded with the same primary amount of the substrate, malononitrile and MeOH. Further reaction runs were performed in the same manner at room temperature.

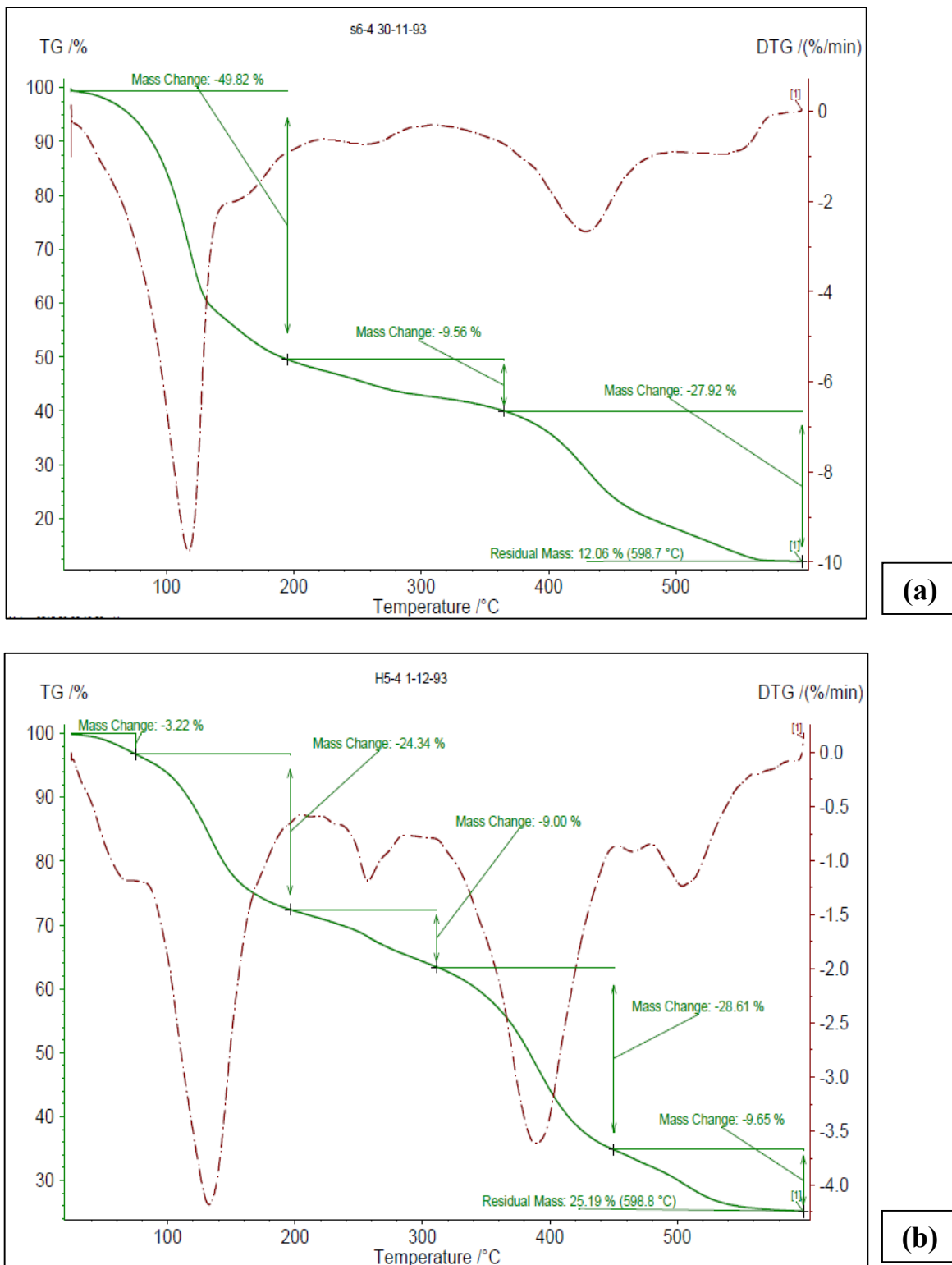


Figure S1. Thermogravimetric analysis of TMU-25 (a) and TMU-26 (b).

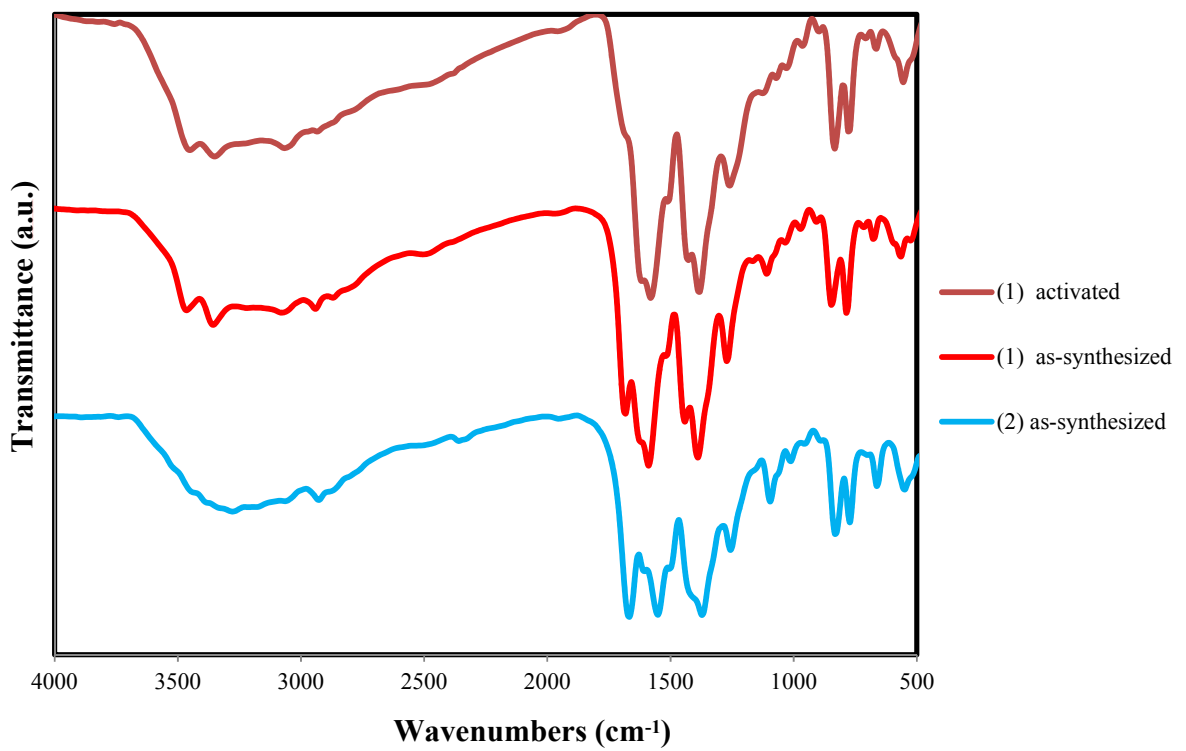


Figure S2. FT-IR spectra of TMU-25 (1) and TMU-26 (2)

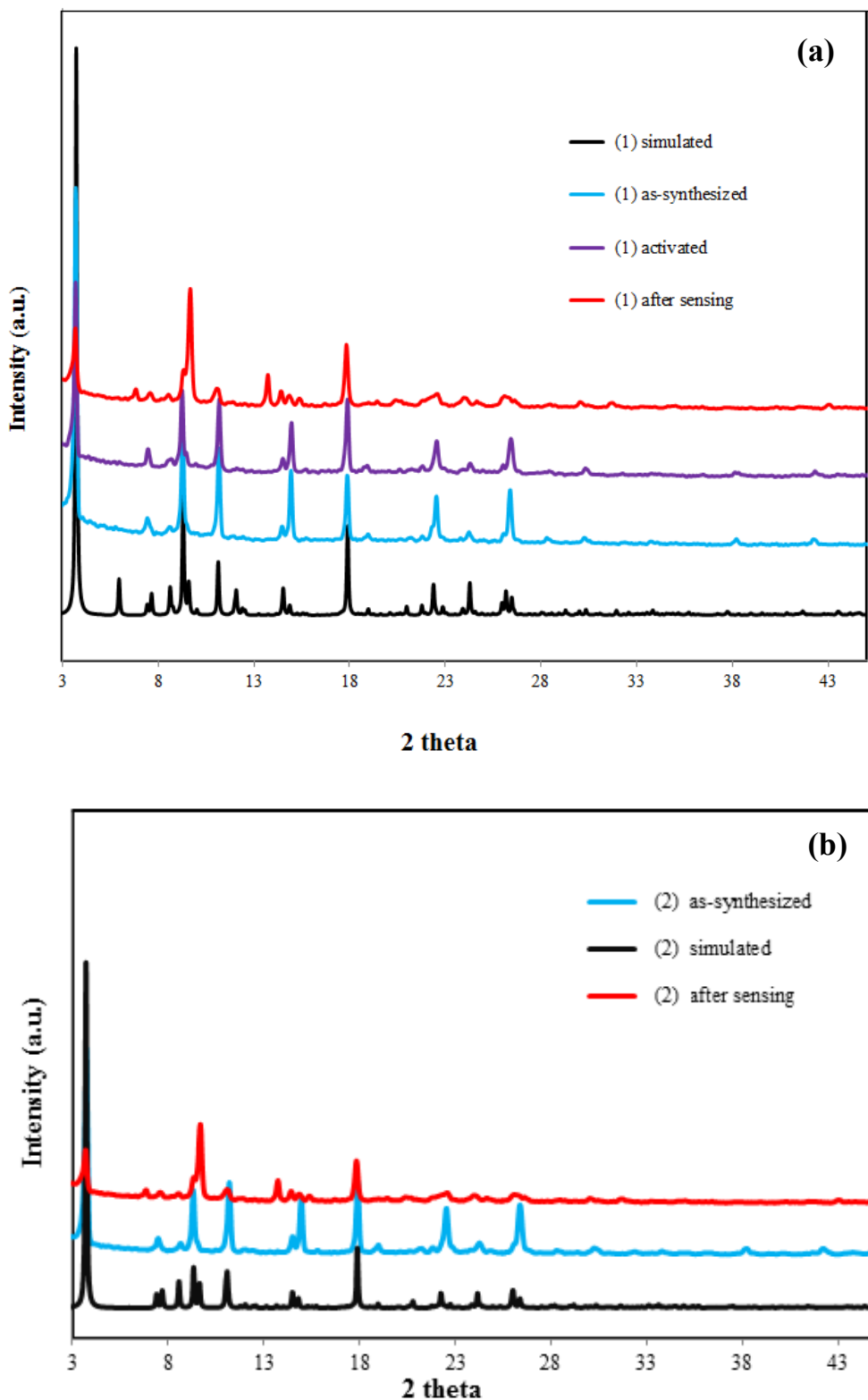


Figure S3. PXRD patterns of simulated, as-synthesized, activated and after sensing of TMU-25 (a) and TMU-26 (b).

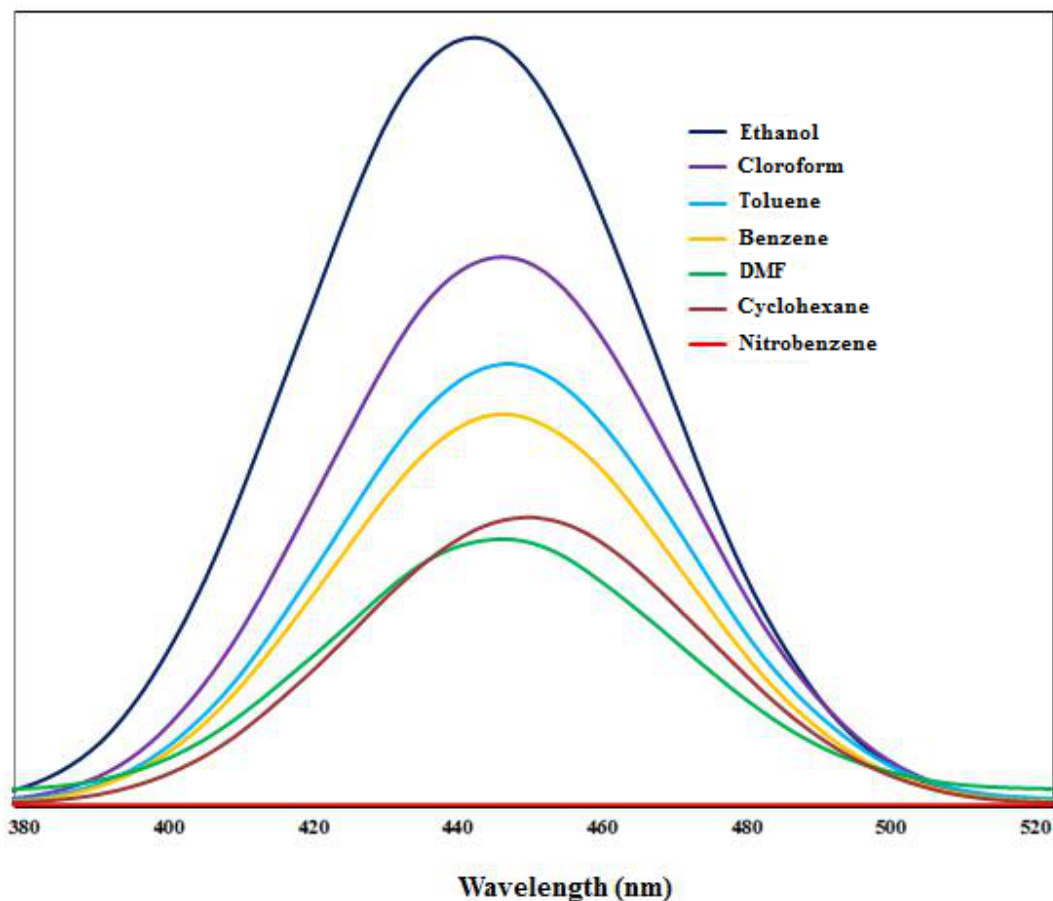


Figure S4. Fluorescence emission spectra of TMU-25 dispersed in different solvents, excited at 336 nm.

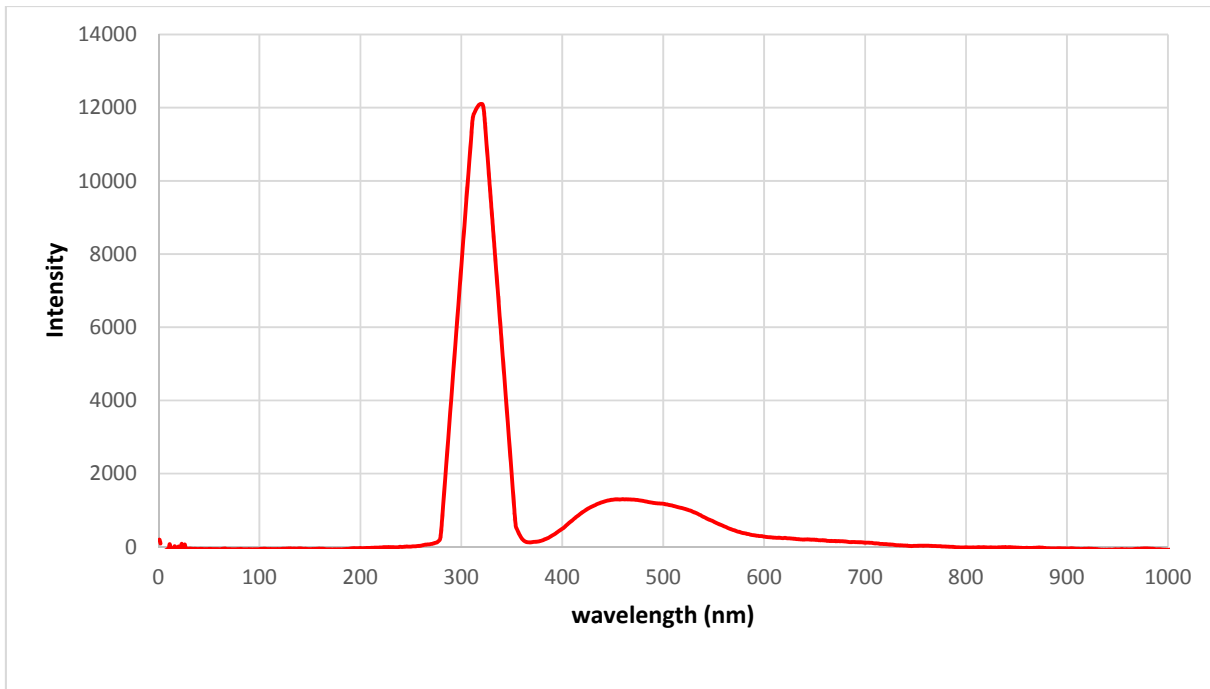


Figure S5. The solid photoluminescence spectra of TMU-25

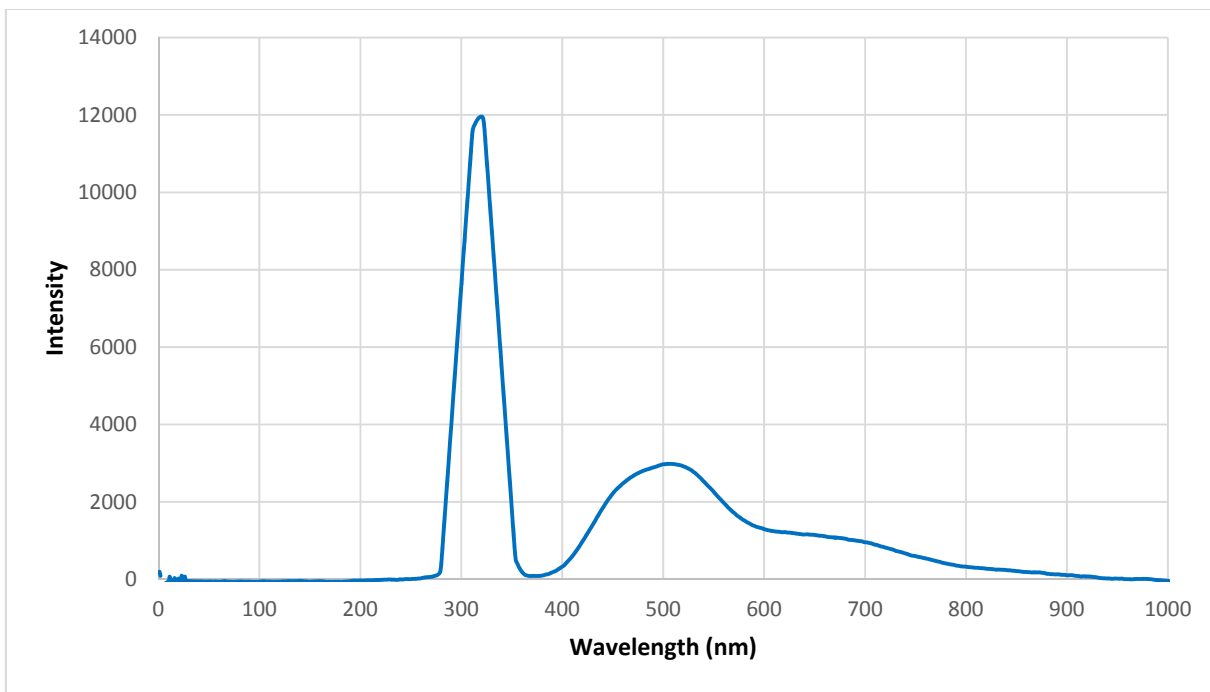


Figure S6. The solid photoluminescence spectra of TMU-26

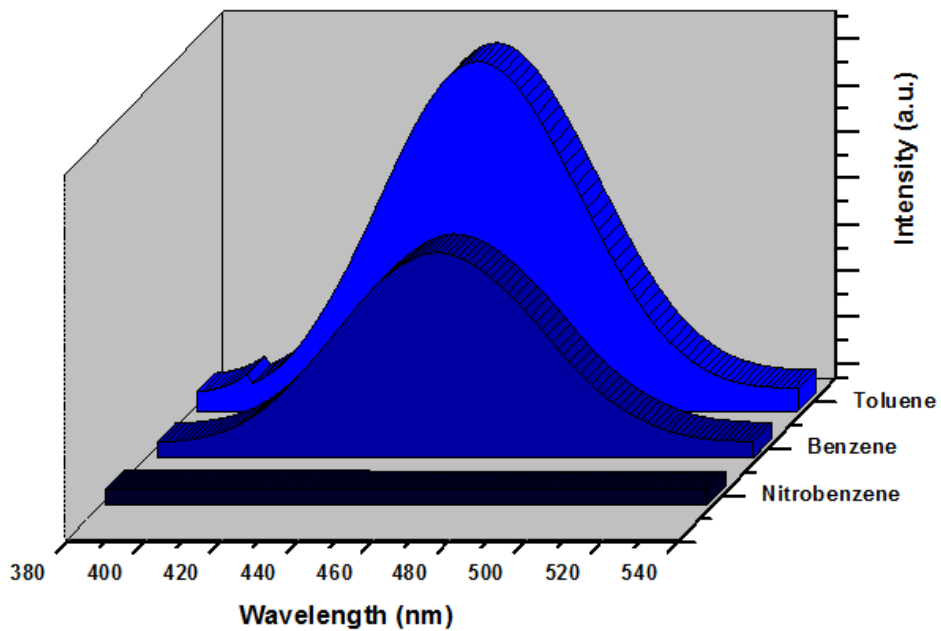


Figure S7. Fluorescence emission spectra of TMU-25 dispersed in nitrobenzene, toluene and benzene, excited at 336 nm.

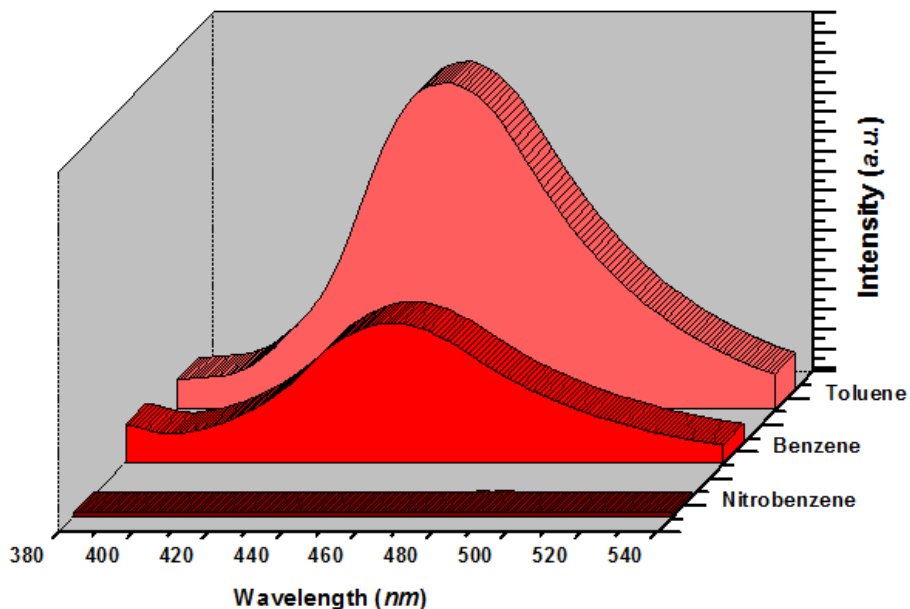


Figure S8. Fluorescence emission spectra of TMU-26 dispersed in nitrobenzene, toluene and benzene, excited at 345 nm.

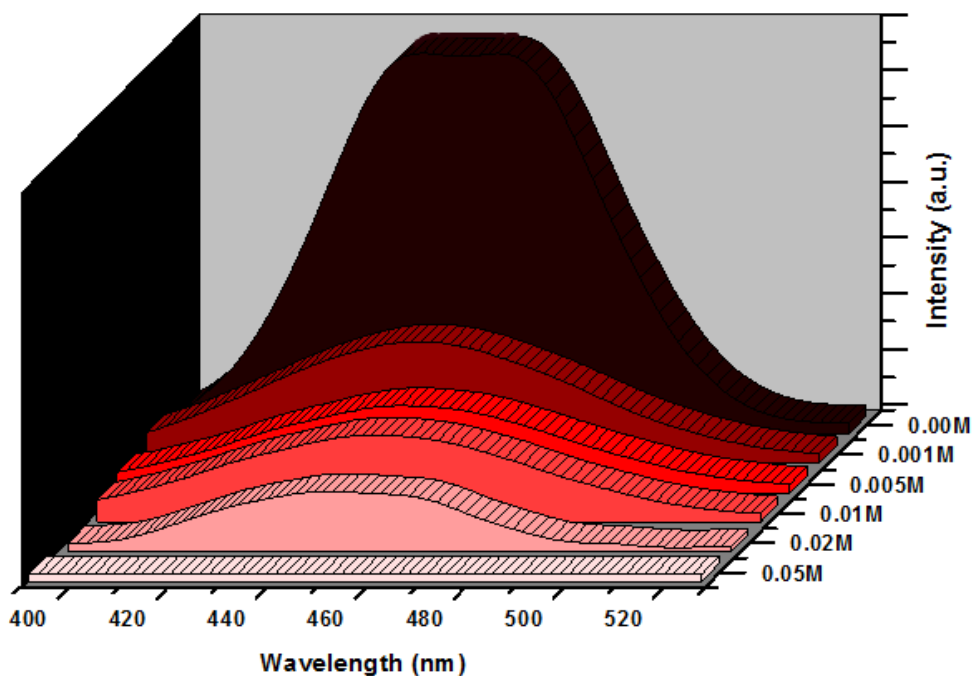


Figure S9. Fluorescence emission spectra of **TMU-25** dispersed in PhCH₃ at different nitrobenzene concentrations, excited at 336 nm.

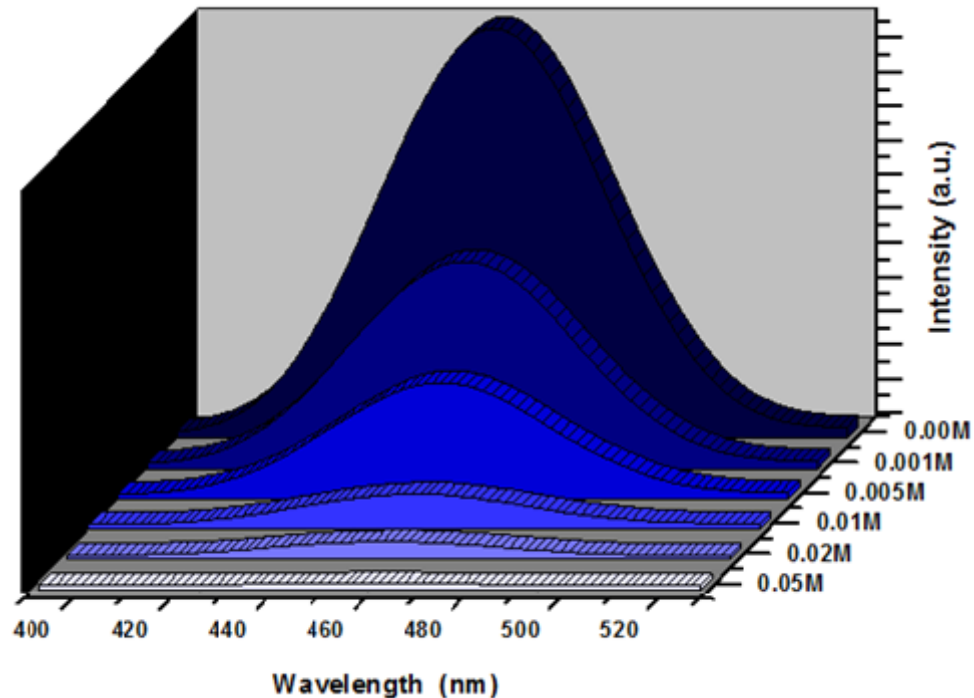


Figure S10. Fluorescence emission spectra of **TMU-26** dispersed in PhCH₃ at different nitrobenzene concentrations, excited at 345 nm.

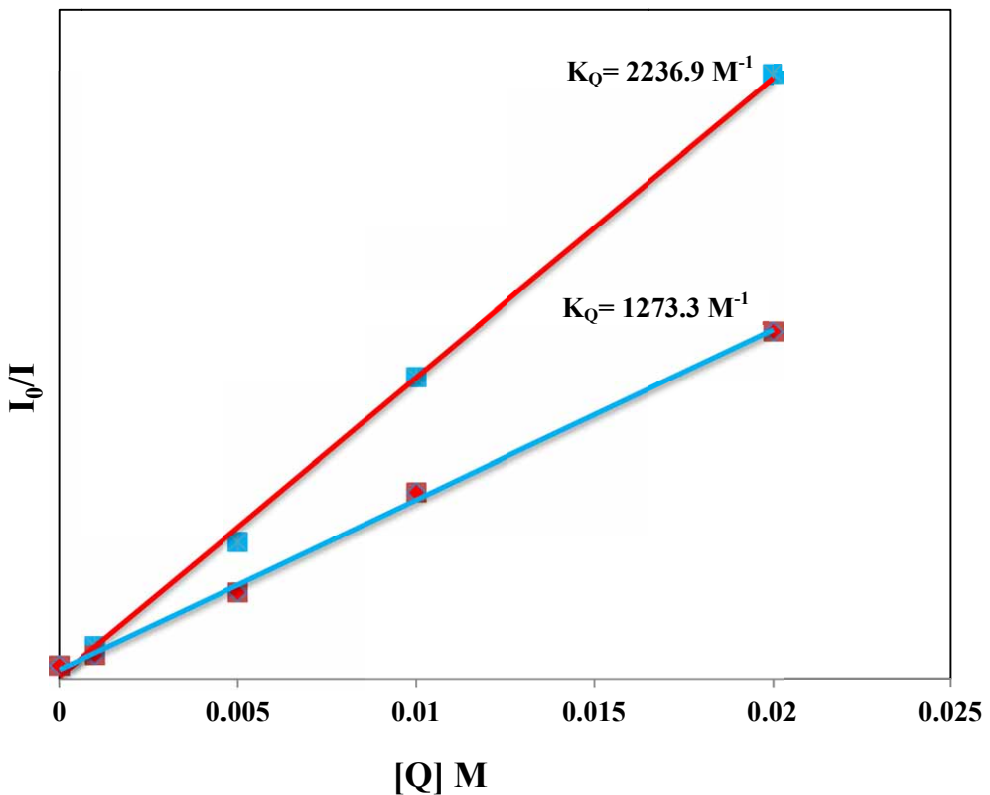


Figure S11. Comparison of Stern–Volmer (SV) plots in the presence of 1 mg of TMU-25 (1) and TMU-26 (2) in different nitrobenzene concentrations ($[Q]$) in toluene.

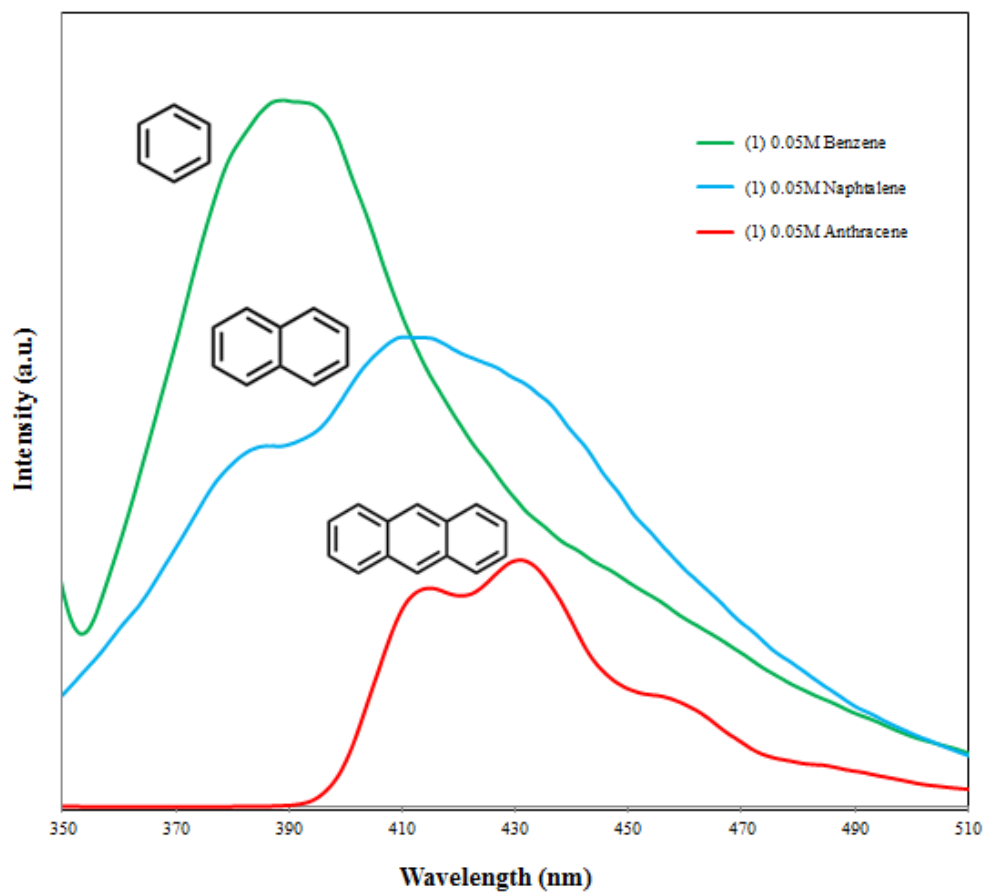


Figure S12. Fluorescence emission spectra of TMU-25 in the presence of different PAHs (0.05M).

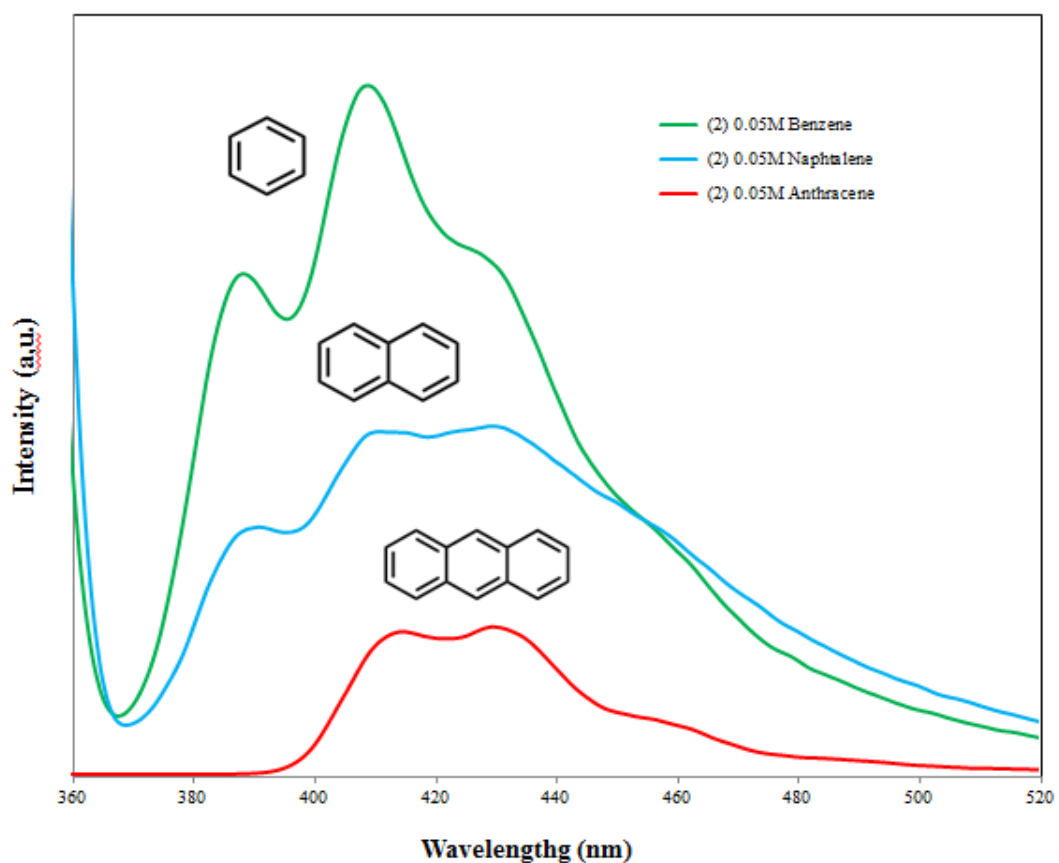


Figure S13. Fluorescence emission spectra of TMU-26 in the presence of different PAHs (0.05M).

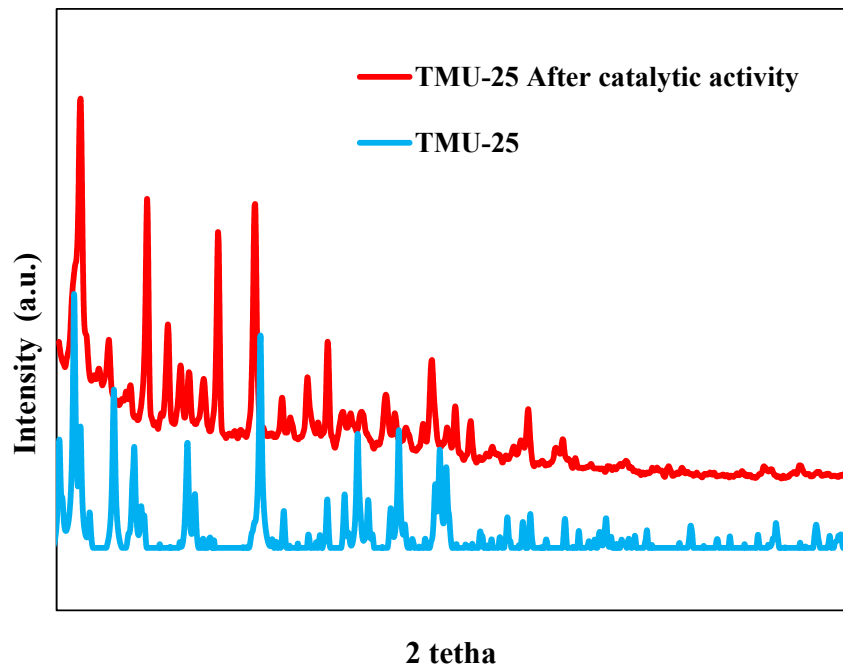


Figure S14. Comparative PXRD patterns of **TMU-25** as-synthesized and the recycled one after the condensation reaction.

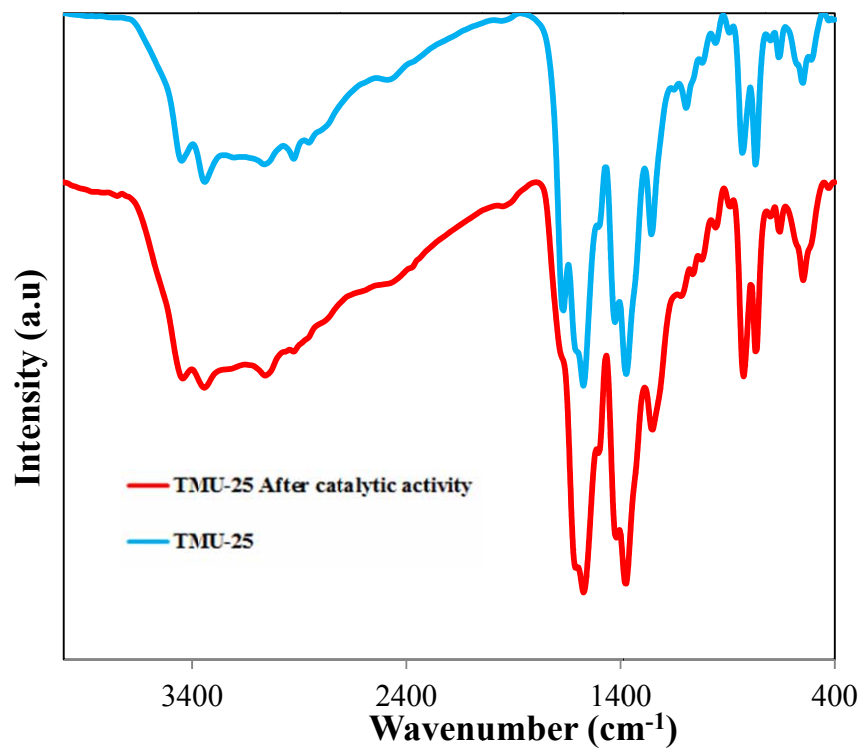


Figure S15. Comparative FT-IR spectra of **TMU-25** as-synthesized and the recycled one after the condensation reaction.

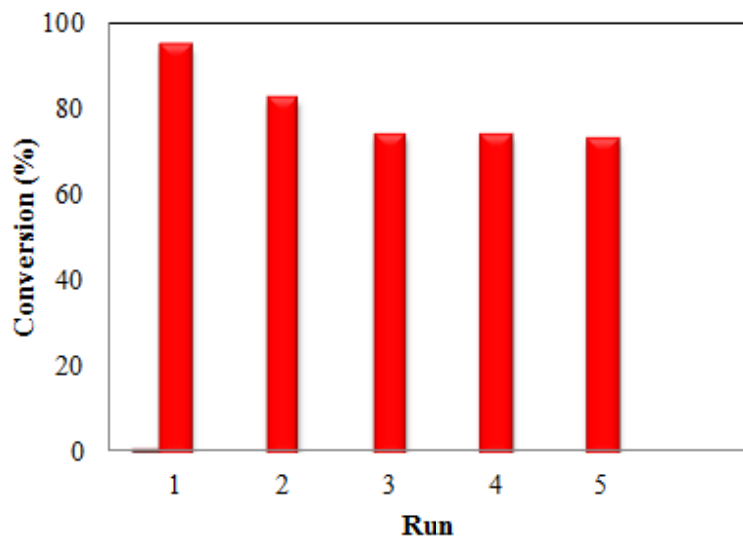


Figure S16. Reusability of **TMU-25** in Knoevenagel condensation reaction. (Conditions: catalyst (5 mol%), benzaldehyde (2 mmol), malononitril (2.1 mmol), MeOH, 30 min, room temperature)

Table S1. π - π stacking interactions between parallel L pillar ligands coordinated to two adjacent metal centers in TMU-25 and TMU-26

π-interactions	TMU-25	TMU-26
$\pi_{\text{py}}\text{-}\pi_{\text{py}}$ stacking	3.7891(5), 3.8336(6) Å	3.7591(11), 3.8400(11) Å 3.7854(11), 3.8365(11) Å
$\pi_{\text{ph}}\text{-}\pi_{\text{ph}}$ stacking	4.1578(6), 4.0123(6) Å	4.1782(12), 4.0663(11) Å 4.0168(11), 4.1370(12) Å

Table S2. Relative contributions of various non-covalent contacts to the Hirshfeld surface area in compounds TMU-25 and TMU-26.

Compound	H···H	C···H	C···C	N···H	O···H	metal···O	metal···N
TMU-25	42.6	21.7	7.1	5.2	8.9	4.0	2.5
TMU-26	41.9	25.1	2.9	6.2	9.9	4.9	12.5

References

- [1] T. M. McPhillips, S. E. McPhillips, H. J. Chiu, A. E. Cohen, A. M. Deacon, P. J. Ellis, E. Garman, A. Gonzalez, N. K. Sauter, R. P. Phizackerley, S. M. Soltis, P. J. Kuhn, *Synchrotron Rad.* 2002, 9, 401-406.
- [2] W. Kabsch, *J. Appl. Cryst.* 1993, 26, 795-800.
- [3] G. M. Sheldrick, *SHELXL-97* Program for crystal structure refinement, University of Gottingen, Germany, 1997.
- [4] L. J. Barbour, *J. Supramol. Chem.* 2001, 1, 189-191.
- [5] O. V. Dolomanov, L. J. Bourhis, R. J. Gildea, J. A. K. Howard, H. Puschmann, *J. Appl. Cryst.* 2009, 42, 339-341.